



HAL
open science

**MOFs by Transformation of 1D-Coordination Polymers
II: The Homoleptic Divalent Rare Earth
3D-Benzotriazolate $3\infty[\text{Eu}(\text{Btz})_2]$ Initiating from
 $1\infty[\text{Eu}(\text{Btz})_2(\text{BtzH})_2]$**

Jens-Christoph Rybak, Inga Schellenberg, Rainer Pöttgen, Klaus
Mueller-Buschbaum

► **To cite this version:**

Jens-Christoph Rybak, Inga Schellenberg, Rainer Pöttgen, Klaus Mueller-Buschbaum. MOFs by Transformation of 1D-Coordination Polymers II: The Homoleptic Divalent Rare Earth 3D-Benzotriazolate $3\infty[\text{Eu}(\text{Btz})_2]$ Initiating from $1\infty[\text{Eu}(\text{Btz})_2(\text{BtzH})_2]$. Journal of Inorganic and General Chemistry / Zeitschrift für anorganische und allgemeine Chemie, 2010, 636 (9-10), pp.1720. 10.1002/zaac.201000077 . hal-00552460

HAL Id: hal-00552460

<https://hal.science/hal-00552460>

Submitted on 6 Jan 2011

HAL is a multi-disciplinary open access archive for the deposit and dissemination of scientific research documents, whether they are published or not. The documents may come from teaching and research institutions in France or abroad, or from public or private research centers.

L'archive ouverte pluridisciplinaire **HAL**, est destinée au dépôt et à la diffusion de documents scientifiques de niveau recherche, publiés ou non, émanant des établissements d'enseignement et de recherche français ou étrangers, des laboratoires publics ou privés.



**MOFs by Transformation of 1D-Coordination Polymers II:
The Homoleptic Divalent Rare Earth 3D-Benzotriazolates
 $^3_{\infty}[\text{Eu}(\text{Btz})_2]$ Initiating from $^1_{\infty}[\text{Eu}(\text{Btz})_2(\text{BtzH})_2]$**

Journal:	<i>Zeitschrift für Anorganische und Allgemeine Chemie</i>
Manuscript ID:	zaac.201000077
Wiley - Manuscript type:	Article
Date Submitted by the Author:	05-Feb-2010
Complete List of Authors:	Rybak, Jens-Christoph; Ludwig-Maximilians Universitaet Muenchen, Department Chemie Schellenberg, Inga; Westfälische Wilhelms Universität, Institut für Anorganische und Analytische Chemie Pöttgen, Rainer; Westfälische Wilhelms Universität, Institut für Anorganische und Analytische Chemie Mueller-Buschbaum, Klaus; Ludwig-Maximilians Universitaet Muenchen, Department Chemie
Keywords:	MOFs, Coordination Polymers, Lanthanides, Benzotriazolates, Crystal structure



MOFs by Transformation of 1D-Coordination Polymers II:

The Homoleptic Divalent Rare Earth 3D-Benzotriazolate ${}^3[\text{Eu}(\text{Btz})_2]$ Initiating from ${}^1[\text{Eu}(\text{Btz})_2(\text{BtzH})_2]$

Jens-Christoph Rybak^a, Inga Schellenberg^b, Rainer Pöttgen^b and Klaus Müller-Buschbaum^{a,*}

^a München, Department Chemie der Ludwig-Maximilians-Universität

^b Münster, Institut für Anorganische und Analytische Chemie der Westfälischen Wilhelms Universität

Dedicated to Professor Bernd Harbrecht on the Occasion of his 60th Birthday

Received...

Abstract. The solvent free reaction route produces coordination polymers that have a dimensionality of the linkage which is increasing with the thermal energy. The synthesis of the 3D MOF structure ${}^3[\text{Eu}(\text{Btz})_2]$ marks the final thermal reaction step within the system europium/1*H*-1,2,3-benzotriazole. It can be obtained by a reaction of the metal with a melt of benzotriazole above 230 °C or from thermal treatment of the 1D coordination polymer ${}^1[\text{Eu}(\text{Btz})_2(\text{BtzH})_2]$, $\text{Btz}^- = 1,2,3\text{-benzotriazolate anion}$, $\text{C}_6\text{H}_4\text{N}_3^-$, $\text{BtzH} = 1\text{H-}1,2,3\text{-benzotriazole}$, $\text{C}_6\text{H}_5\text{N}_3$, which is formed first at about 100 °C from the same reagents. In addition to the trivalent rare earth ions it can thus be shown that also divalent Eu^{II} together with benzotriazole exhibits transformation of a 1D coordination polymer into a 3D MOF. The homoleptic framework ${}^3[\text{Eu}(\text{Btz})_2]$ exhibits a high thermal stability (525 °C) for an exothermically decomposing coordination compound. As ${}^3[\text{Eu}(\text{Btz})_2]$ is always obtained as a microcrystalline product, structure solution and refinement were achieved by X-ray powder techniques.

1
2
3 For further characterization ^{151}Eu -Mössbauer, IR and Raman spectroscopy as well as micro
4
5 and thermal analysis were carried out.
6
7
8
9

10 **Keywords:** MOFs; Coordination Polymers; Lanthanides; Benzotriazoles; Crystal structure
11

12
13
14

* Priv.-Doz. Dr. Klaus Müller-Buschbaum
15 Department Chemie
16 Ludwig-Maximilians-Universität München
17 Butenandtstraße 5-13(D)
18 81377 München
19 Germany
20 Fax: 0049 89 2180 77851
21 E-Mail: Klaus.Mueller-Buschbaum@cup.uni-muenchen.de
22
23
24
25
26

27 Introduction

28
29 The synthesis of oxygen-free lanthanide coordination compounds like amides and amine do-
30 nor complexes can be achieved via the reaction of metals with a self-consuming melt of an
31 amine under solvent free conditions [1 - 3]. The utilization of an organic melt replaces the
32 solvent. We successfully elaborated this synthesis strategy for lanthanide metals and observed
33 a general trend towards the formation of coordination polymers. Several exhibit a 1D chain-
34 like linkage [4], including the benzotriazolate ligand [5]. Depending on the coordination
35 modes of the ligands also 2D and 3D amide frameworks are observed [6 - 7]. Thus this syn-
36 thesis strategy is also a suitable approach to the chemistry of MOFs (Metal Organic Frame-
37 works) [8, 9]. Here the 4f elements can play an important role because of luminescence as an
38 intrinsic property of the frameworks [10, 11]. Due to the oxophilicity of the rare earth ele-
39 ments oxygen-free MOFs are rarely found in the literature. As the ligand 1*H*-1,2,3-
40 benzotriazole is commercially used as an UV absorber [12], we consider it interesting as
41 linker in MOF frameworks. For the trivalent lanthanides we could show that strand-like coor-
42 dination polymers of the formula $^1_{\infty}[\text{Ln}(\text{Btz})_3(\text{L})]$ [5], Ln = La - Yb, Btz^- = benzotriazolate
43
44
45
46
47
48
49
50
51
52
53
54
55
56
57
58
59
60

1
2
3 anion, $C_6H_4N_3^-$, $L = NH_3$, Py, BtzH, $Ph(NH_2)_2$, transform upon release of L into homoleptic
4
5 3D MOF structures of the formula $^3_\infty[Ln(Btz)_3]$ [13]. Thus also 3D-frameworks are accessible
6
7
8 from BtzH. We can now expand this on the divalent state, as europium shows transformation
9
10 of the 1D polymer $^1_\infty[Eu(Btz)_2(BtzH)_2]$ into the homoleptic framework $^3_\infty[Eu(Btz)_2]$. It retains
11
12 the divalent state and is not oxidized.
13
14
15
16
17
18

19 Experimental

20 All manipulations were carried out under inert atmospheric conditions using glove-box, am-
21
22 poule as well as vacuum line techniques. The IR spectra were recorded using a BRUKER
23
24 FTIR-IS66V-S spectrometer, the Raman spectra using a BRUKER FRA 106-S spectrometer.
25
26 For the IR investigations KBr pellets were used under vacuum. The thermal properties were
27
28 studied using multiple simultaneous DTA/TG experiments (SETARAM TG-DTA 92-16): on
29
30 the reaction of europium metal with benzotriazole, on single crystalline $^1_\infty[Eu(Btz)_2(BtzH)_2]$
31
32 and on $^3_\infty[Eu(Btz)_2]$. All samples were heated from 20 °C up to 1000 °C in a constant He flow
33
34 of 50 ml/min. 3.7 mg Eu and 15.3 mg BtzH were treated at a heating rate of 5 °C/min, 17.1
35
36 mg of crystalline $^1_\infty[Eu(Btz)_2(BtzH)_2]$ as well as 17.2 mg $^3_\infty[Eu(Btz)_2]$ were treated at a heating
37
38 rate of 10 K/min. The micro analysis was carried out on a ELEMENTAR Vario El analyser.
39
40
41
42
43
44
45
46
47
48

49 *Synthesis of $^3_\infty[Eu(Btz)_2]$ (I)*

50
51 a) $^1_\infty[Eu(Btz)_2(BtzH)_2]$ (248 mg = $4.0 \cdot 10^{-4}$ mol) was sealed in an evacuated two-chamber
52
53 DURAN glass ampoule and the substance chamber heated within 3 h to 350 °C in a tube oven.
54
55 The other chamber was positioned outside the oven so that the temperature gradient to room
56
57 temperature led to condensation of the released ligand in the second chamber. The tempera-
58
59 ture was held for 72 h and then cooled to room temperature within 3 h. The reaction gave 153
60

1
2
3 mg (0.39 mmol, 98 %) of a yellow-orange powder product of **1**. The reaction product showed
4
5 a very small amount of black impurities most probably originating from decomposition of the
6
7 released BtzH molecules.
8
9

10
11 **b)** Europium (76 mg = $5 \cdot 10^{-4}$ mol), 1H-benzotriazole (BtzH, $C_6H_5N_3$; 179 mg = $1.5 \cdot 10^{-3}$ mol),
12
13 and Hg (20 mg) were sealed in an evacuated DURAN glass ampoule. The reaction mixture
14
15 was heated within 23 h to 230 °C. The temperature was held for 120 h. The melt was cooled to
16
17 80 °C within 150 h and to room temperature in another 24 h. The reaction gave 178 mg (0.46
18
19 mmol, 92 %) of a yellow-orange powdery product of **1** with a small amount of a black de-
20
21 composition product.
22
23

24
25 Anal. calc. $C_{12}H_8EuN_6$ ($M = 388.20 \text{ g mol}^{-1}$) C, 37.13 %; H, 2.08. Found: C, 37.5; H, 2.1.
26
27

28 **MIR** (KBr): (3061.6 w, 2258.2 vw, 1611.3 w, 1573.8 w, 1483.9 m, 1447.1 m, 1392.6 w,
29
30 1282.4 m, 1260.3 m, 1163.1 m, 144.0 vs, 1124.0 s, 993.2 w, 984.7 w, 912.4 m, 778.9 s, 744.3
31
32 vs, 694.0 m, 632.2 m, 546.7 m, 477.8 vw, 438.1 w, 418.5 w) cm^{-1} .
33
34

35 **RAMAN**: (3063.0 w, 1572.3 w, 1448.6 vw, 1393.1 w, 1283.6 vw, 1165.4 vw, 1138.9 vw,
36
37 1029.2 w, 780.8 w, 633.9 vw) cm^{-1} .
38
39
40
41

42 **Synthesis of** ${}^1_{\infty}[Eu(Btz)_2(BtzH)_2]$ (**2**)

43
44 The synthesis of ${}^1_{\infty}[Eu(Btz)_2(BtzH)_2]$ was carried out according to [5c]. Anal. calc.
45
46 $C_{24}H_{18}N_{12}Eu$ ($M = 626.45 \text{ g mol}^{-1}$) C, 46.02; N, 26.83; H, 2.90. Found: C, 45.8; N, 26.9; H,
47
48 3.0. For **MIR** spectroscopy see also [5c].
49
50
51
52
53
54
55

56 **Crystal Structure Determination**

57
58 A powder sample of ${}^3_{\infty}[Eu(Btz)_2]$ (**1**) was prepared for X-ray powder diffraction analy-
59
60 sis under glove-box conditions and sealed in a glass capillary of 0.3 mm diameter. The data

1
2
3 collection was carried out on a STOE STADI P X-Ray diffractometer (Mo $K_{\alpha 1}$ radiation
4
5 70.93171(4) pm, Ge-111 monochromator, Debye-Scherrer geometry) at 297 K. The structure
6
7 was determined with the program package TOPAS ACADEMIC 4.1 [14] using the charge
8
9 flipping algorithm of *Sütő* and *Oszlányi* [15] after intensity extraction with the Pawley-method
10
11 [16]. Rietveld refinements for compound **1** were done with the TOPAS package, using the
12
13 fundamental parameters approach for reflection profiles (convolution of appropriate source
14
15 emission profiles with axial instrument contributions as well as crystallite microstructure
16
17 effects). Preferred orientation of the crystallites was described with a spherical harmonics
18
19 function of 8th order. ${}^3[\text{Eu}(\text{Btz})_2]$ crystallises in the cubic space group $Fd\bar{3}m$. The integrity of
20
21 symmetry and geometry were checked using the program PLATON [17] that resulted in the
22
23 addressed space group subsequent to an initial solution in the space group $Fd\bar{3}$. The diffracto-
24
25 grams were checked for crystal systems of lower symmetry on a possible splitting of reflec-
26
27 tions and half widths of the reflections counter checked with the fit of the structure refine-
28
29 ment, both giving no sign on a different crystal system. The Eu atoms were refined isotropi-
30
31 cally. Displacement parameters for the C and N atoms were refined isotropically using a con-
32
33 straint for all atoms of one element, thus refining one parameter for the displacement param-
34
35 eters of each element. H atoms have not been put into consideration in this structure refine-
36
37 ment. The results from the powder diffraction data in their present state give a complete de-
38
39 scription of the crystal structure of ${}^3[\text{Eu}(\text{Btz})_2]$, however crystallinity of the product does not
40
41 yet allow a refinement of final contentment regarding the weighted Durbin-Watson figure of
42
43 merit and a less constraint refinement of displacement parameters. Crystallographic data are
44
45 summarised in Table 1, Figure 1 shows measured and calculated diffractograms of **1**, as well
46
47 as their difference plot. The crystal structure of **2** was already determined on single crystals
48
49 [5c]. The chain structure crystallizes in the monoclinic space group $C2/c$. Further information
50
51 was deposited at the Cambridge Crystallographic Data Centre, CCDC, 12 Union Road, Cam-
52
53
54
55
56
57
58
59
60

1
2
3 bridge CB2 1EZ, UK (fax: +44 1223336033 or e-mail: deposit@ccdc.cam.ac.uk) and may be
4
5 requested by citing the deposition number CCDC-xxxx, the names of the authors and the lit-
6
7 erature citation.
8
9

10 11 12 13 ***Mössbauer spectroscopy***

14
15 The 21.53 keV transition of ^{151}Eu with an activity of 130 MBq (2 % of the total activity of a
16
17 $^{151}\text{Sm}:\text{EuF}_3$ source) was used for the Mössbauer spectroscopic experiment, which was con-
18
19 ducted in the usual transmission geometry. The measurement was performed with a commer-
20
21 cial helium-bath cryostat. The temperature of the absorber was kept at 77 K, while the source
22
23 was kept at room temperature. The temperature was controlled by a resistance thermometer
24
25 (± 0.5 K accuracy). The sample was enclosed in a small glass container at a thickness corre-
26
27 sponding to about 15 mg of the Mössbauer active element/cm². 62.5 mg of **1** were used for the
28
29 Mössbauer spectroscopic experiments equalling about 25 mg of Eu.
30
31
32
33
34
35
36
37
38
39

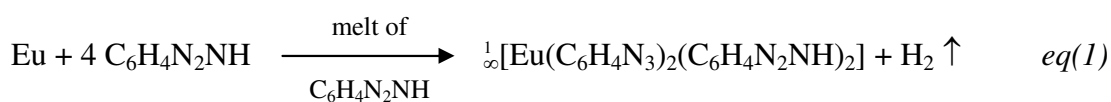
40 **Discussion**

41 42 ***Synthesis and Thermal Properties***

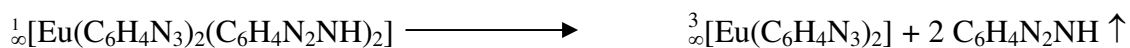
43
44 The solvent free melt synthesis utilizing metals is a redox reaction that also produces hydro-
45
46 gen gas [3]. The metals are oxidized by the amine melt giving amides [1 - 4]. In order to keep
47
48 the reaction temperatures in the range of the stability region of organic materials, amalgam
49
50 activation is mostly suitable [1 - 7, 18]. If the thermal stabilities of the amine ligands is not
51
52 sufficient, several other activation methods like the use of electrides [19] or microwaves [2e]
53
54 can also be applied.
55
56
57

58
59 As we have previously shown that benzotriazolates of the lanthanides obtained from reactions
60
of the metals with a self-consuming melt of the ligand constitute of one-dimensional coordina-

1
2
3 tion polymers [5]. We elaborated that the thermal treatment can also lead to partial decompo-
4
5 sition of the benzotriazole ring system, so that next to 1*H*-benzotriazole molecules products
6
7 from the melt decomposition like NH₃ and Ph(NH₂)₂ are formed and incorporated into the
8
9 coordination sphere of the rare earth ions as co-ligands L in $^1_{\infty}[\text{Ln}(\text{Btz})_3(\text{L})]$ [5]. The possible
10
11 exchange of these neutral ligands vs. other amine bases such as pyridine [5b] as well as the
12
13 thermal plateau subsequent to the release of the coordinating ligands BtzH = L in the thermal
14
15 investigation of $^1_{\infty}[\text{Ce}(\text{Btz})_3(\text{BtzH})]$ [5a] gave rise to the question, what happens to the strand
16
17 structures upon removal of the non-backbone ligands. The answer is the formation of frame-
18
19 work structures for both trivalent [13] and divalent lanthanides, presented here. Though endo-
20
21 thermic, the benzotriazole release is too rapid to grow single crystals of $^3_{\infty}[\text{Ln}(\text{Btz})_{2-3}]$ by heat-
22
23 ing, also if carried out with low heating rates. For the trivalent strands $^1_{\infty}[\text{Ln}(\text{Btz})_3(\text{BtzH})]$ reac-
24
25 tions in solvothermal pyrrole conformed the thermal formation of $^3_{\infty}[\text{Ln}(\text{Btz})_3]$ [13] as they
26
27 yield single crystalline material. The simulated powder patterns are identical to the decompo-
28
29 sition products of $^1_{\infty}[\text{Ln}(\text{Btz})_3(\text{BtzH})]$. However, for divalent $^1_{\infty}[\text{Eu}(\text{Btz})_2(\text{BtzH})_2]$ this treatment
30
31 does not give crystals of suitable size. Accordingly, only microcrystalline material of the prod-
32
33 uct of the benzotriazole release is available. Due to advances in the structure solution and re-
34
35 finement from powders, it is possible to present a structure solution here that corroborates the
36
37 results of the other analysis methods and the formula $^3_{\infty}[\text{Eu}(\text{Btz})_2]$, and that also contains diva-
38
39 lent europium. The formation of homoleptic $^3_{\infty}[\text{Eu}(\text{Btz})_2]$ (**1**) from $^1_{\infty}[\text{Eu}(\text{Btz})_2(\text{BtzH})_2]$ (**2**) can
40
41 be described as a condensation reaction under release of coordinating 1*H*-BtzH ligands as neu-
42
43 tral N donor molecules.
44
45
46
47
48
49
50
51
52
53
54
55
56



>200 °C



eq(2)

From the thermal investigations that utilize simultaneous DTA/TG an identification of the signals is possible by comparison of investigations on the reaction of europium metal with benzotriazole, on single crystalline ${}^1_{\infty}[\text{Eu}(\text{Btz})_2(\text{BtzH})_2]$ (**2**) and on the MOF ${}^3_{\infty}[\text{Eu}(\text{Btz})_2]$ (**1**). Figure 2 displays the results of simultaneous DTA/TG on the respective samples.

In the thermal investigation of the reaction itself signal (1) indicates the melting point of the ligand benzotriazole (96 °C; expected mp. 97 - 99 °C). Signal (2) starts directly afterwards and addresses to the endothermic reaction of BtzH and Eu, followed by signal (3) that indicates evaporation of excess BtzH. Signals (4) and (5) at 230 °C and 255 °C can be identified with the transformation of ${}^1_{\infty}[\text{Eu}(\text{Btz})_2(\text{BtzH})_2]$ into ${}^3_{\infty}[\text{Eu}(\text{Btz})_2]$ under release of two equivalents of BtzH. Signal (6) indicates exothermic decomposition of the ${}^3_{\infty}[\text{Eu}(\text{Btz})_2]$ framework under release of N₂ at 525 °C.

The thermal investigation on ${}^1_{\infty}[\text{Eu}(\text{Btz})_2(\text{BtzH})_2]$ (**2**) consequently shows only the signals (4 – 6) starting with the two step release of benzotriazole, the temperatures matching with the reaction DTA/TG. The mass loss in the TG experiment is 36.5 % equalling two BtzH equivalents (expected 37.7 %). Finally, the thermal investigation on ${}^3_{\infty}[\text{Eu}(\text{Btz})_2]$ (**1**) only exhibits the final exothermic decomposition step (6).

Thereby thermal formation of ${}^3_{\infty}[\text{Eu}(\text{Btz})_2]$ from ${}^1_{\infty}[\text{Eu}(\text{Btz})_2(\text{BtzH})_2]$ also matches with the formation of ${}^3_{\infty}[\text{Ln}(\text{Btz})_3]$ from ${}^1_{\infty}[\text{Ln}(\text{Btz})_3(\text{L})]$, if the different valence is taken into account. The thermal stability of ${}^3_{\infty}[\text{Ln}(\text{Btz})_3]$ is 465 °C for La and 470 °C for Ce, and thus lower than of ${}^3_{\infty}[\text{Eu}(\text{Btz})_2]$, their decomposition also being exothermic due to the release of N₂ [13].

Crystal Structure

In contrast to the chain structure of $^1_\infty[\text{Eu}(\text{Btz})_2(\text{BtzH})_2]$ (**2**, see description in [5c]) the crystal structure of $^3_\infty[\text{Eu}(\text{Btz})_2]$ (**1**) is a three-dimensional homoleptic framework structure (see Figure 3). The structure contains two crystallographically independent Eu atoms. Both are octahedrally coordinated by N atoms of six benzotriazolate anions each. The orientations of the six ligands vary for the two Eu sites (see Figure 4). A distinct difference is found for the linkages to other europium atoms. Eu1 is linked to four Eu2 atoms via face connections of four alternating triangular faces of the coordination octahedron giving a tetrahedral arrangement of Eu2 around Eu1. Eu2 is linking to only two Eu1 atoms via the antiprismatic triangular faces of the coordination octahedron resulting in a 180° linkage (see Figures 2 and 4).

Regarding the topology of the framework structure [20] that is depicted in Figure 5, a complicated topology of a 12,12 net results. However it can be described in a simplified way as it originates from the diamond structure of Eu1 atoms as connectivity points. In-between all Eu1 connectivity centres the Eu2 have to be considered as additional connectivity centres. This equals a diamond structure that would have an interstitial atom on each bond. It can also be described in comparison with β -cristobalite with Eu1 taking the positions of the silicon atoms and Eu2 the positions of the oxygen atoms. Therefore a simplified topology symbol is not 6,4 but 12,4 constituted of large twelve-membered rings to three other rings. For a complete consideration of the topology the face connections of the polyhedra can accordingly be addressed as “triple-bridges” [21]. This would enlarge the overall topology to a 12,12 net.

The Eu – N distances are 269.5(11) and 277.4(22) pm which indicates divalent Europium. Eu^{II} – N distances [22] of comparable compounds are e.g. ranging from 260.1(5) to 287.3(6) pm in $^1_\infty[\text{Eu}(\text{Btz})_2(\text{BtzH})_2]$ [5c]. They can spread over a wide range and cover C.N. of Eu between 6 and 12, Eu^{II} – N being 252 – 268 pm in $^1_\infty[\text{Eu}(\text{Cbz})_2]$ [4a], 255 – 257 pm for $[\text{Eu}(\text{Cbz})_2(\text{thf})_4]$

1
2
3 [23], 258 –311 pm for ${}^3_{\infty}[\text{Eu}(\text{Tzpy})_2]$ [7e]. Completed coordination spheres for the europium
4
5
6 atoms are depicted in Figure 6.
7
8
9

12 ${}^{151}\text{Mö}ß\text{bauer Spectroscopy}$

15 The Mössbauer spectrum of compound **1** taken at 77 K is presented in Figure 7 together
16 with transmission integral fits. The corresponding fitting parameters for the main component
17 of the spectrum are an isomer shift $\delta = -12.44(3)$ mm/s, an experimental line width $\Gamma = 4.0(2)$
18 mm/s, and a quadrupole splitting parameter $\Delta E_Q = 3.4(6)$ mm/s. This signal clearly reflects
19 divalent europium. The isomer shift of -12.44 mm/s lies in the range of divalent europium
20 and is comparable to other europium containing metal organic frameworks [7e]. An additional
21 spectral component is detected near 0.8 mm/s, indicating the presence of some Eu^{3+} , most
22 likely due to partial hydrolyses of the sample, leading to europium (III) oxide or hydroxide.
23 This signal was included as a simple Lorentzian in the fit. The resulting ratio of $\text{Eu}^{2+} / \text{Eu}^{3+}$ is
24 83 : 17, respectively.
25
26
27
28
29
30
31
32

33 The experimental line width of 4.0 mm/s of the Eu(II) signal is somewhat high. The broad-
34 ening results from the two crystallographically independent europium sites confirmed by the
35 crystal data. It was not possible to differentiate between these two sites due to their similarity.
36 Summing up, the Mössbauer spectroscopic investigation validates the divalent character of
37 both europium sites.
38
39
40
41
42
43
44

45 **Conclusions**

46
47 Conversion of a 1D-coordination polymer into a 3D-linked MOF is shown by the transforma-
48 tion of ${}^1_{\infty}[\text{Eu}(\text{Btz})_2(\text{BtzH})_2]$ into ${}^3_{\infty}[\text{Eu}(\text{Btz})_2]$. It is the first example for a divalent rare earth ion
49 to show this conversion. The divalence of europium is proven by ${}^{151}\text{Mö}ß\text{bauer}$ spectroscopy.
50
51 The homoleptic framework ${}^3_{\infty}[\text{Eu}(\text{Btz})_2]$ exhibits an exceptionally high thermal stability for an
52 exothermically decomposing coordination compound and MOF structure.
53
54
55
56
57
58
59
60

We gratefully acknowledge the *Deutsche Forschungsgemeinschaft* for supporting this work within a Heisenberg Scholarship and the SPP-1362 MOFs, the support of the *Dr. Otto-Röhm-Gedächtnis foundation* and the *Wilhelm-Klemm foundation*. We thank the *LMU München* and *Prof. Dr. W. Schnick* for the formidable conditions and their support.

References

- [1] a) G. B. Deacon, A. Gitlits, B.W. Skelton, A. H. White, *J. Chem. Soc., Chem. Commun.* **1999**, 1213; b) G. B. Deacon, A. Gitlits, P. W. Roesky, M. R. Bürgstein, K. C. Lim, B. W. Skelton, A. H. White, *Chem. Eur. J.* **2001**, 7, 127; c) G. B. Deacon, C. M. Forsyth, A. Gitlits, B. W. Skelton, A. H. White, *J. Chem. Soc. Dalton Trans.* **2004**, 1239.
- [2] a) K. Müller-Buschbaum, C. C. Quitmann, *Inorg. Chem.* **2003**, 42, 2742; b) C. C. Quitmann, V. Bezugly, F. R. Wagner, K. Müller-Buschbaum, *Z. Anorg. Allg. Chem.* **2006**, 632, 1173; K. Müller-Buschbaum, C. C. Quitmann, *Inorg. Chem.* **2006**, 45, 2678.
- [3] K. Müller-Buschbaum, *Z. Anorg. Allg. Chem.* **2005**, 631, 811.
- [4] a) K. Müller-Buschbaum, C. C. Quitmann, *Z. Anorg. Allg. Chem.* **2003**, 629, 1610; b) C. C. Quitmann, K. Müller-Buschbaum, *Z. Naturforsch.* **2004**, 59b, 562; c) C. C. Quitmann, K. Müller-Buschbaum, *Z. Anorg. Allg. Chem.* **2005**, 631, 1191.
- [5] a) K. Müller-Buschbaum, Y. Mokaddem, *Eur. J. Inorg. Chem.* **2006**, 2000; b) K. Müller-Buschbaum, Y. Mokaddem, *Z. Anorg. Allg. Chem.* **2007**, 633, 513; c) J.-C. Rybak, K. Müller-Buschbaum, *Z. Anorg. Allg. Chem.* **2010**, 636, 126.
- [6] a) K. Müller-Buschbaum, Y. Mokaddem, C. J. Höller, *Z. Anorg. Allg. Chem.* **2008**, 634, 2973; b) C. J. Höller, M. Mai, C. Feldmann, K. Müller-Buschbaum, *J. Chem. Soc. Dalton Trans.* **2010**, DOI:10.1039/b911460b; c) C. C. Quitmann, K. Müller-Buschbaum, *Z. Anorg. Allg. Chem.* **2004**, 630, 573.
- [7] a) K. Müller-Buschbaum, Y. Mokaddem, *J. Chem. Soc. Chem. Commun.* **2006**, 2060; b) K. Müller-Buschbaum, Y. Mokaddem, *Solid State Sci.* **2008**, 416; d) K. Müller-Buschbaum, *Z. Naturforsch.* **2006**, 61b, 792; e) K. Müller-Buschbaum, Y. Mokaddem, F. Schappacher, R. Pöttgen, *Angew. Chem. Int. Ed.* **2007**, 46, 4385, *Angew. Chem.*

- 1
2
3
4
5
6
7
8
9
10
11
12
13
14
15
16
17
18
19
20
21
22
23
24
25
26
27
28
29
30
31
32
33
34
35
36
37
38
39
40
41
42
43
44
45
46
47
48
49
50
51
52
53
54
55
56
57
58
59
60
- 2007**, *119*, 4463; f) A. Zurawski, J. Sieler, K. Müller-Buschbaum, *Z. Anorg. Allg. Chem.* **2009**, *635*, 2034.
- [8] a) N. L. Rosi, J. Eckert, M. Eddaoudi, D. T. Vodak, J. Kim, M. O’Keeffe, O. M. Yaghi, *Science* **2003**, *300*, 1127; b) B. Kesanli, Y. Cui, M. R. Smith, E.W. Bittner, B. C. Bockrath, W. Lin, *Angew. Chem. Int. Ed.* **2005**, *44*, 72, *Angew. Chem.* **2005**, *117*, 74; c) J. L. C. Rowsell, A. R. Millward, K. S. Park *J. Am. Chem. Soc.* **2004**, *126*, 5666; d) H. Furukawa, M. A. Miller, O. M. Yaghi, *J. Mater. Chem.* **2007**, *17*, 3197; e) T. Loiseau, C. Serre, C. Haugeunard, G. Fink, G. Taulelle, M. Henry, T. Bataille, G. Ferey, *Chem. Eur. J.* **2004**, *10*, 1373; f) B. Panella, M. Hirscher, H. Pütter, U. Müller, *Adv. Funct. Mater.* **2006**, *16*, 520; g) H. Althues, S. Kaskel, *Langmuir* **2002**, *18*, 7428; h) M. O’Keeffe, O. M. Yaghi, *Nature* **1999**, *402*, 276; i) G. Ferey, *Chem. Mater.* **2001**, *13*, 3084.
- [9] a) S. R. Batten, R. Robson, *Angew. Chem. Int. Ed. Engl.* **1998**, *37*, 1460; b) A. J. Blake, N. R. Champness, P. Hubberstey, W. S. Li, M. A. Withersby, M. Schröder, *Coord. Chem. Rev.* **1999**, *183*, 117; c) P. J. Hagrman, D. Hagrman, J. Zubieta, *Angew. Chem. Int. Ed.* **1999**, *38*, 2638, *Angew. Chem.* **1999**, *111*, 2850; d) M. Eddaoudi, J. Kim, J. B. Wachter, H. K. Chae, M. O’Keeffe, O. M. Yaghi, *J. Am. Chem. Soc.* **2001**, *123*, 4368; e) I. Senkovska, S. Kaskel, *Eur. J. Inorg. Chem.* **2006**, *22*, 4564.
- [10] a) D.-L. Long, A. J. Blake, N. R. Champness, C. Wilson, M. Schröder, *J. Am. Chem. Soc.* **2001**, *123*, 3401; b) D.-L. Long, A. J. Blake, N. R. Champness, C. Wilson, M. Schröder, *Angew. Chem. Int. Ed.* **2001**, *40*, 2444; c) L. Pan, N. Zheng, Y. Wu, S. Han, R. Yang, X. Huang, J. Li, *Inorg. Chem.* **2001**, *40*, 828; d) R. Cao, D. F. Sun, Y. C. Liang, M. C. Hong, K. Tatsumi, Q. Shi, *Inorg. Chem.* **2002**, *41*, 2087; e) T. M. Reineke, M. Eddaoudi, M. Fehr, D. Kelley, O. M. Yaghi, *J. Am. Chem. Soc.* **1999**, *121*, 1651; f) Y. Kim, D.-Y. Jung, *J. Chem. Soc., Chem. Commun.* **2002**, 908; g) X. Zheng, C. Sun, S. Lu, F. Liao, S. Gao, L. Jin, *Eur. J. Inorg. Chem.* **2004**, 3262; h) J. Liu, E. A. Meyer, J. A. Cowan, S. G. Shore, *Chem. Soc., Chem. Commun.* **1998**, 2043.
- [11] K. Müller-Buschbaum, S. Gomez-Torres, P. Larsen, C. Wickleder, *Chem. Mater.* **2007**, *19*, 65.
- [12] a) BASF Technical Information, *Uvinul Lichtschutzmittel*, EVP 004605 d, **2005**; b) UMID, UmweltMedizinischerDienst, *Abschlussbericht zur multizentrischen MCS-Studie*, Bundesamt für Strahlenschutz, Umwelt Bundesamt, **2005**.
- [13] K. Müller-Buschbaum, Y. Mokaddem, *Z. Anorg. Allg. Chem.* **2008**, *634*, 2360.

- 1
2
3 [14] A. Coelho, TOPAS-Academic, version 4.1, Coelho Software, Brisbane **2007**.
4
5 [15] G. Oszlányi, A. Sütő, *Acta Cryst.* 2004, *A60*, 134.
6
7 [16] G. S. Pawley, *J. Appl. Cryst.* **1981**, *14*, 357.
8
9 [17] A. L. Spek, PLATON-2000, *A Multipurpose Crystallographic Tool;V1.07*, University
10 of Utrecht **2003**.
11
12 [18] B. Magyar, *Inorg. Chem.* **1968**, *7*, 1457.
13
14 [19] a) C. C. Quitmann, K. Müller-Buschbaum, *Angew. Chem.* **2004**, *116*, 6120; *Angew.*
15 *Chem. Int Ed. Engl.* **2004**, *43*, 5994; b) K. Müller-Buschbaum, *Z. Anorg. Allg. Chem.*
16 **2004**, *630*, 895; c) C. C. Quitmann, K. Müller-Buschbaum, *Z. Anorg. Allg. Chem.*
17 **2004**, *630*, 2422; d) K. Müller-Buschbaum, C. C. Quitmann, A. Zurawski, *Monatshefte*
18 *Chemie/Chemistry Monthly*, **2007**, *138*, 813; e) K. Müller-Buschbaum, *Z. Anorg. Allg.*
19 *Chem.* **2007**, *633*, 1403.
20
21 [20] A. F. Wells, *Three-dimensional nets and polyhedra*, Wiley-Interscience, New York
22 **1977**.
23
24 [21] D.-L. Long, A. J. Blake, N. R. Champness, C. Wilson, M. Schröder, *Angew. Chem.,*
25 *Int. Ed.* **2001**, *40*, 2444; *Angew. Chem.* **2001**, *113*, 2510.
26
27 [22] R. D. Shannon, *Acta Crystallogr. A*, **1976**, *32*, 751.
28
29 [23] G. B. Deacon, C. M. Forsyth, B. M. Gatehouse, P. A. White, *Aust. J. Chem.* **1990**, *43*,
30 795.
31
32
33
34
35
36
37
38
39
40
41
42
43
44

45 Legends for Figures

46
47
48

49 **Figure 1** X-ray powder diffraction diffractogram of **1**. Experimental data are displayed in
50 black, calculated in grey. Difference plot and reflex position markers are displayed below.
51
52

53
54
55 **Figure 2** Simultaneous DTA/TG investigation of the reaction of Eu with BtzH (top), of
56 $^1[\text{Eu}(\text{Btz})_2(\text{BtzH})_2]$ (middle) and of $^3[\text{Eu}(\text{Btz})_2]$ (bottom). Signal (1) indicates the melting
57 point of BtzH, signal (2) belongs to the endothermic reaction of BtzH and Eu, (3) indicates
58
59
60

1
2
3 evaporation of excess BtzH, signals (4) and (5) can be identified with the transformation of
4
5 $^1_\infty[\text{Eu}(\text{Btz})_2(\text{BtzH})_2]$ into $^3_\infty[\text{Eu}(\text{Btz})_2]$ under release of two equivalents of BtzH. Signal (6) in-
6
7
8 dicates exothermic decomposition of the $^3_\infty[\text{Eu}(\text{Btz})_2]$ framework under release of N_2 .
9

10
11
12
13 **Figure 3** Crystal structure of $^3_\infty[\text{Eu}(\text{Btz})_2]$ as a depiction of the coordination polyhedra with a
14
15 view along [110] (top) and [001] (bottom). Eu atoms are displayed in grey, N atoms in dark
16
17 and C atoms in light grey. Edges of the polyhedra do not represent bonds.
18
19
20

21
22
23 **Figure 4** The coordination spheres of the atoms Eu1 and Eu2 in $^3_\infty[\text{Eu}(\text{Btz})_2]$ as a depiction of
24
25 the coordination polyhedra.
26
27

28
29
30 **Figure 5** Schematic drawing of the network topology of $^3_\infty[\text{Eu}(\text{Btz})_2]$ (**1**).
31
32

33
34
35 **Figure 6** The complete coordination spheres and linkage of Eu1 and Eu2 in **1**. Symmetry
36
37 Operations: I: $x, \frac{3}{4} - y, \frac{3}{4} - z$; II: $\frac{3}{4} - y, z, \frac{3}{4} - x$; III: $y, \frac{3}{4} - z, \frac{3}{4} - x$; IV: $z, \frac{3}{4} - x, \frac{3}{4} - y$; V: $\frac{3}{4} - z,$
38
39 $\frac{3}{4} - x, y$; VI: $\frac{3}{4} - x, \frac{3}{4} - y, z$; VII: $\frac{3}{4} - x, y, \frac{3}{4} - z$; VIII: y, z, x ; IX: $\frac{3}{4} - y, \frac{3}{4} - z, x$; X: $-x, -z, -y$;
40
41
42
43 XI: $-x, \frac{1}{4} + z, \frac{1}{4} + y$; XII: $-y, -x, -z$; XIII: $\frac{1}{4} + y, -x, \frac{1}{4} + z$; XIV: z, x, y ; XV: $\frac{3}{4} - z, x, \frac{3}{4} - y$;
44
45 XVI: $\frac{1}{4} + z, \frac{1}{4} + y, -x$; XVII: $-z, -y, -x$.
46
47

48
49 **Figure 7** Experimental and simulated ^{151}Eu Mössbauer spectrum of **1** at 77 K.
50
51
52
53
54
55
56
57
58
59
60

Table 1. Crystallographic data for ${}^3\text{[Eu(Btz)}_2\text{]} (\mathbf{1})$. Standard deviations are given in parentheses.

Formula	$\text{C}_{12}\text{H}_8\text{EuN}_6$
Formula weight [g/mol]	388.20
Crystal system, space group	cubic, $Fd\bar{3}m$
Lattice parameter [pm]	$a = 1994.3(1)$
Cell volume [nm^3]	7931(1)
Z	24
Density [g/cm^3]	1.91
μ [cm^{-1}]	51.9
X-ray radiation	Mo- $\text{K}_{\alpha 1}$, $\lambda = 70.93171(4)$ pm
Diffractometer	STOE STADI P
d range	1.27670 – 11.51392
Data Points	3000
Reflections	123
Refined parameters	38
R_p	0.0703
wR_p	0.0933
R_{bragg}	0.0442
χ^2	1.915
Wght. Durbin-Watson	0.435

Table 2. Selected interatomic distances (in pm) and angles between atoms of ${}^3[\text{Eu}(\text{Btz})_2]$ (1).

Standard deviations are given in parentheses. Symmetry Operations: II: $\frac{3}{4} - y, z, \frac{3}{4} - x$; IV: $z, \frac{3}{4} - x, \frac{3}{4} - y$; VI: $\frac{3}{4} - x, \frac{3}{4} - y, z$; VIII: y, z, x ; X: $-x, -z, -y$; XII: $-y, -x, -z$; XIV: z, x, y ; XVII: $-z, -y, -x$.

Eu1–N1	277.4(22)	N1–Eu1–N1 ^{II/IV/VIII/XIV}	90
Eu2–N2	269.5(11)	N1–Eu1–N1 ^{VI}	180
Eu1–Eu2	431.0(1)	N2–Eu2–N2 ^X	180
		N2–Eu2–N2 ^{XIV/XVII}	85.7(6)
		N2–Eu2–N2 ^{VIII/XII}	94.3(6)

Figure 1

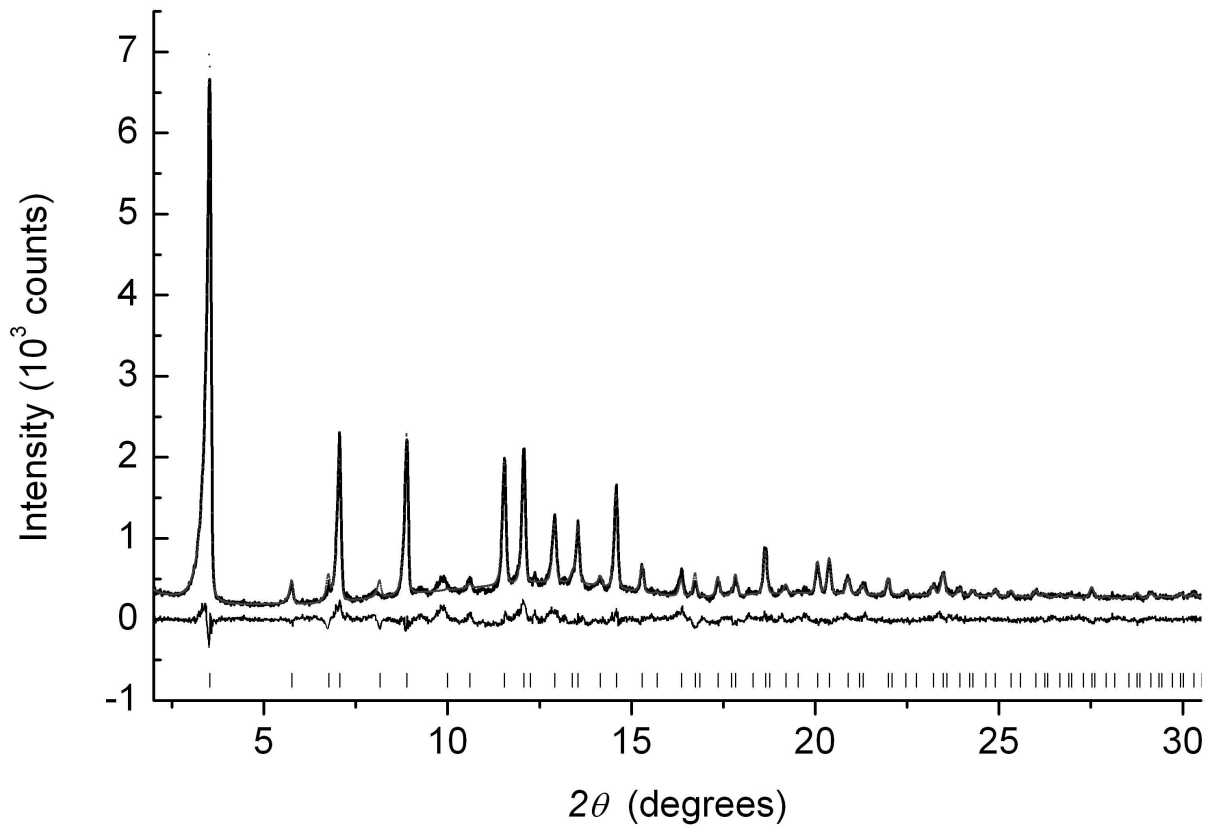


Figure 2

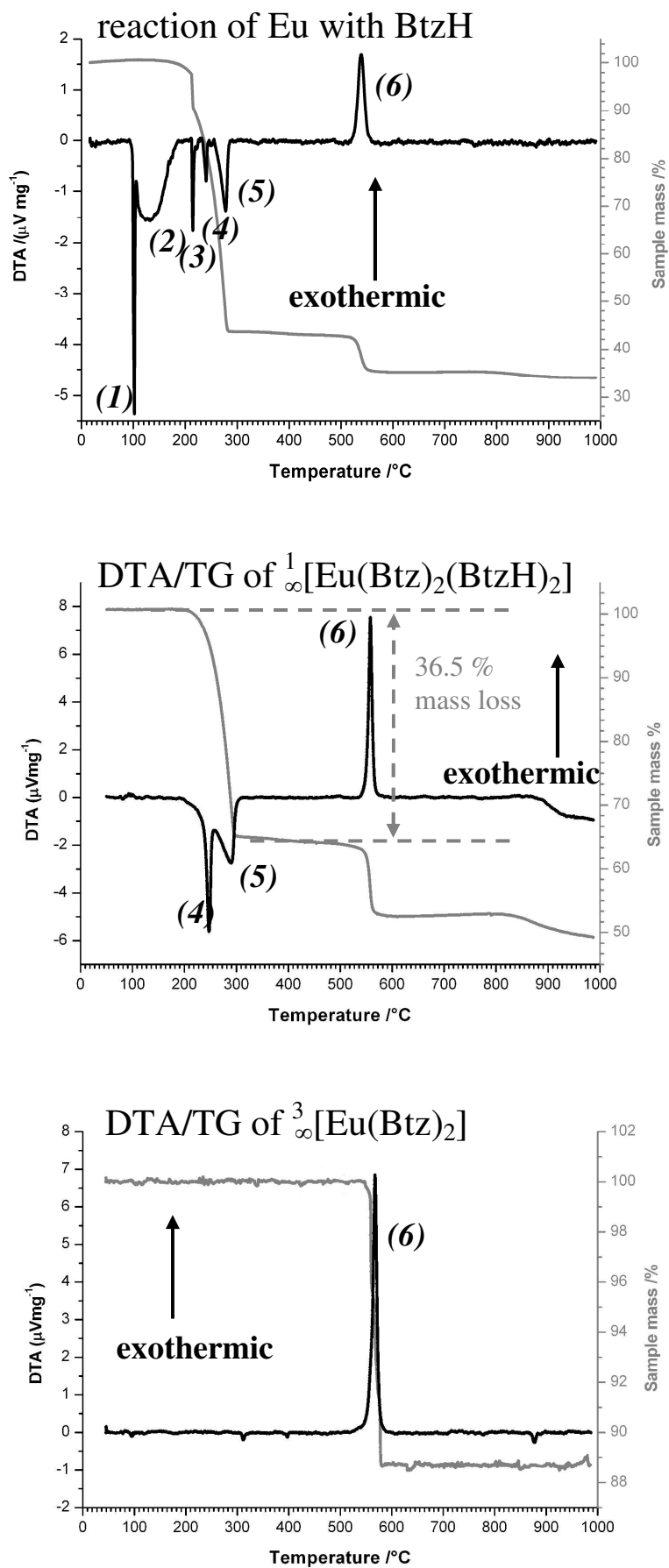


Figure 3

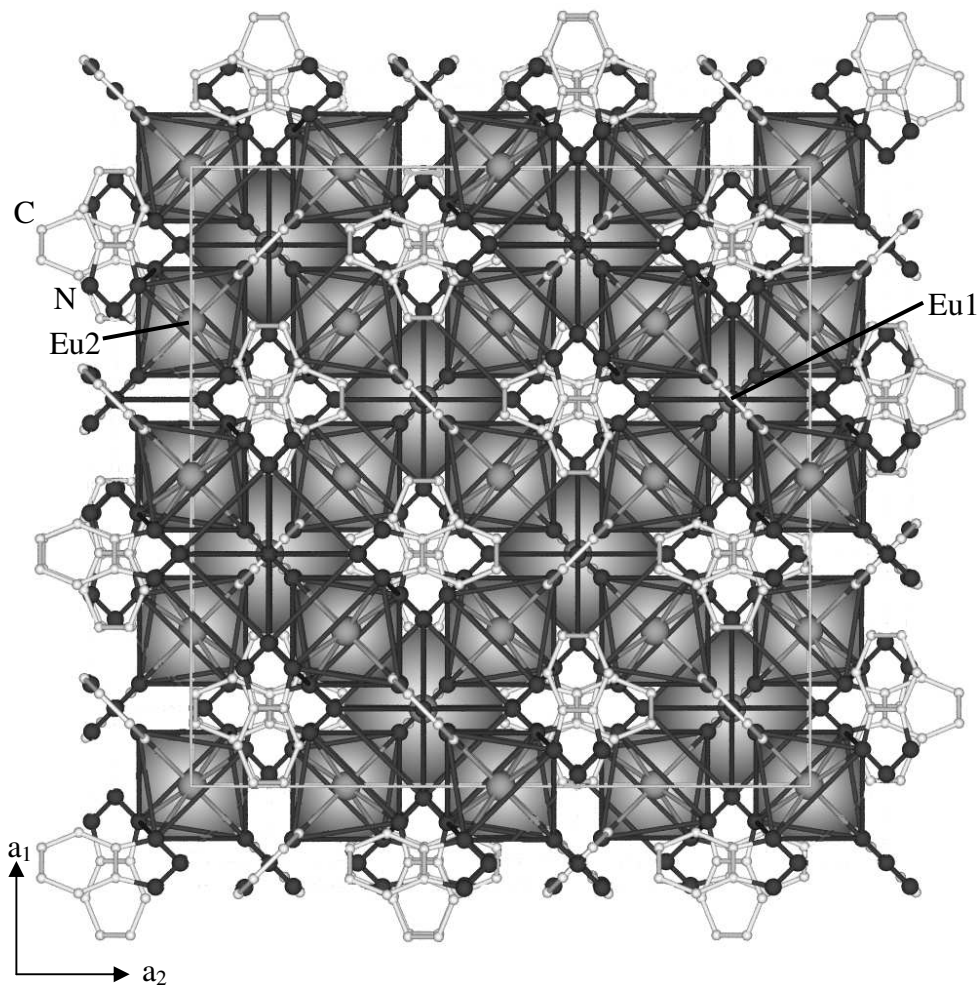
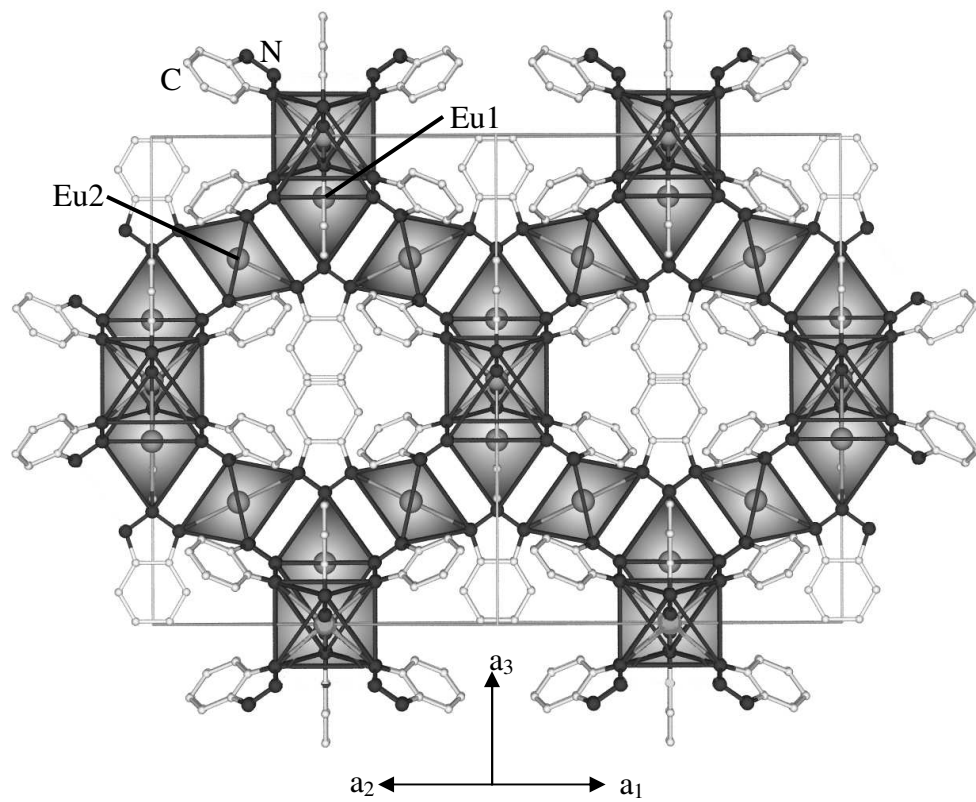


Figure 4

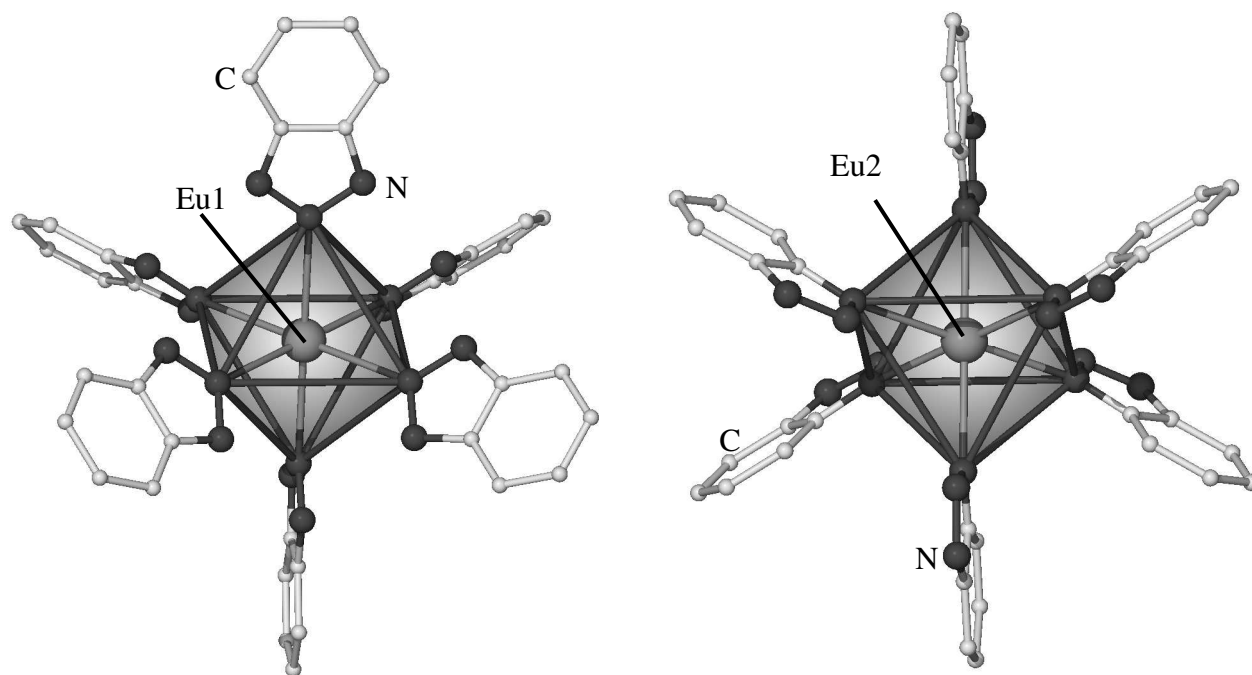


Figure 5

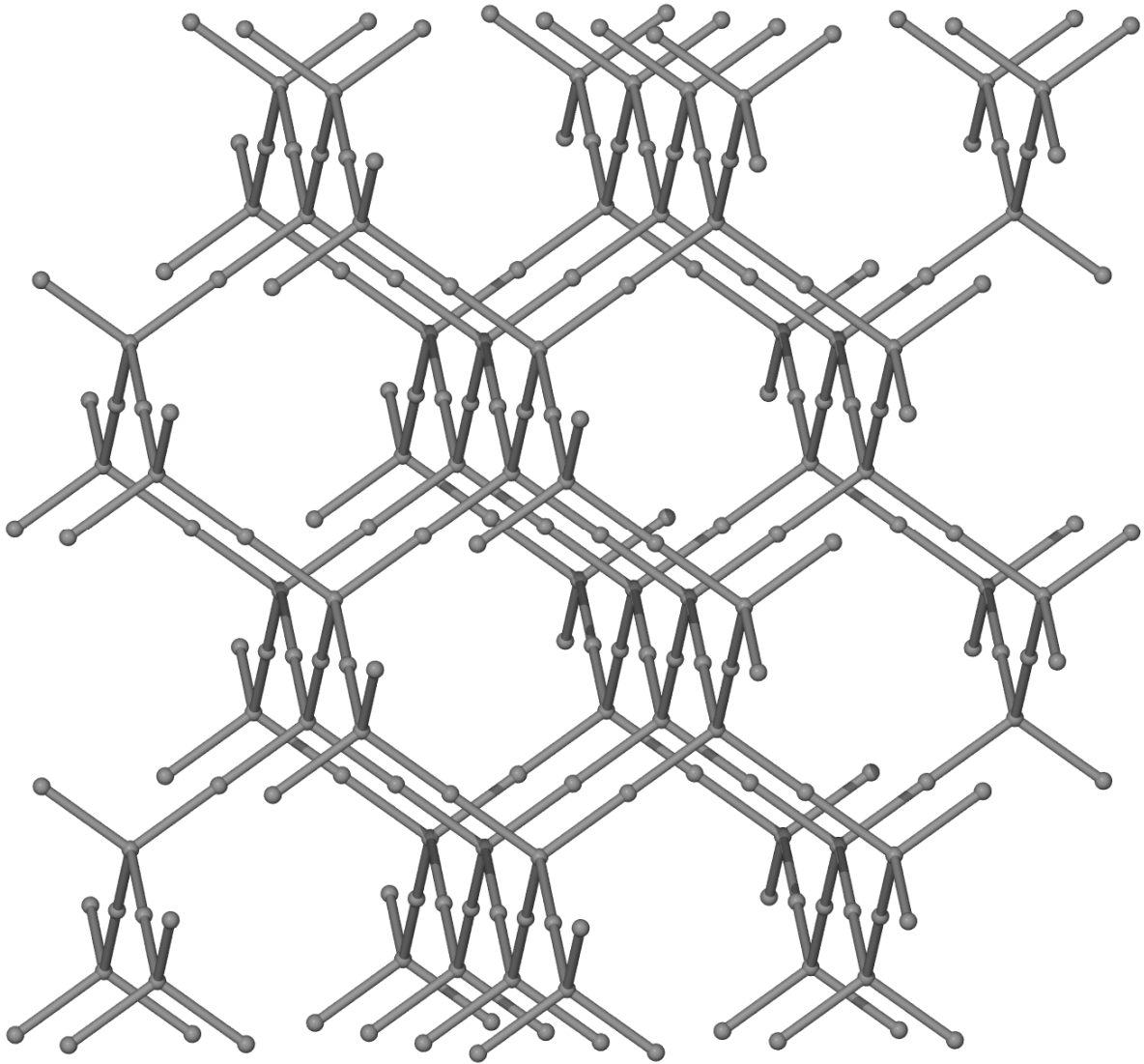


Figure 6

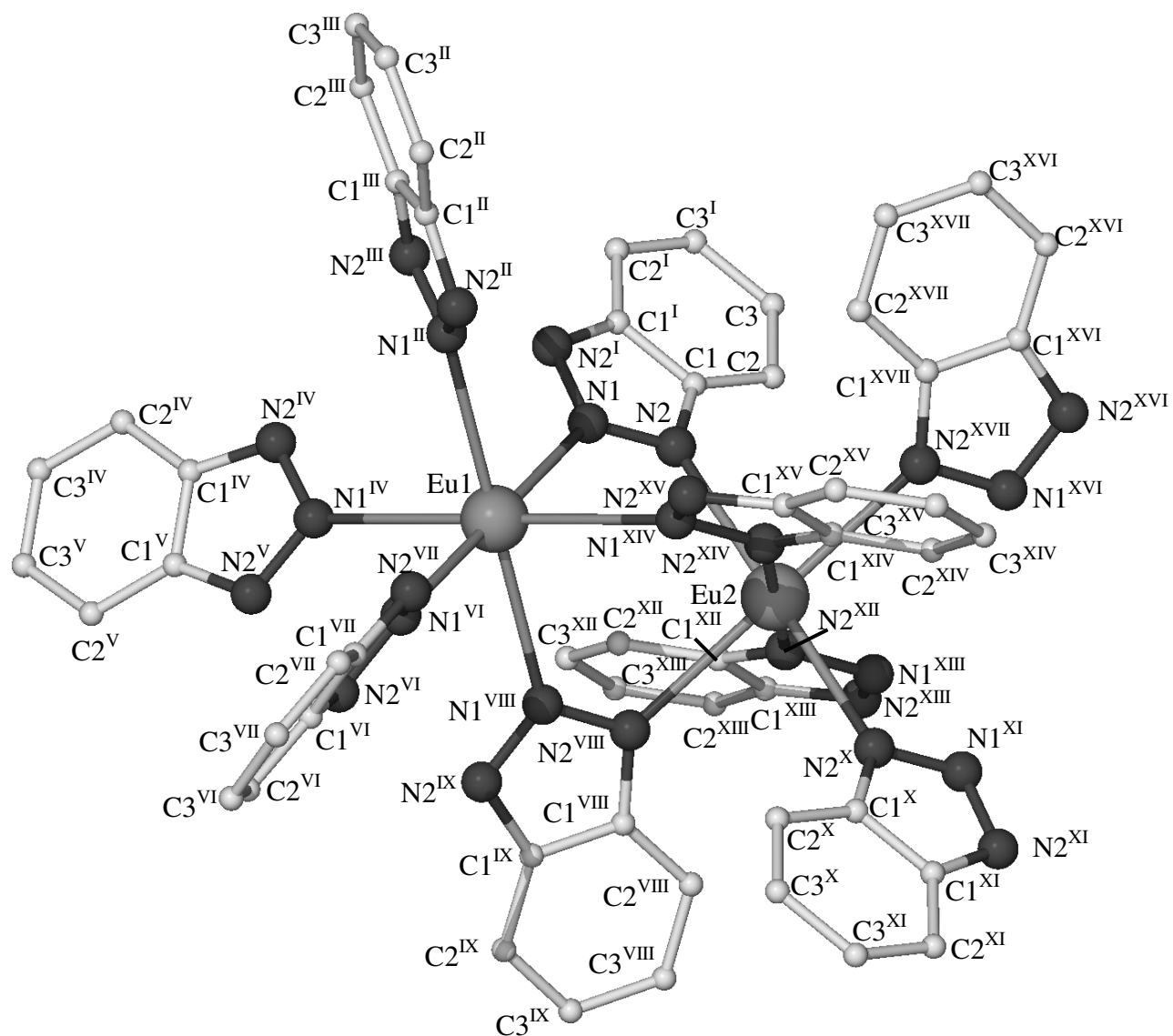


Figure 7

